 DOI: 10.1002/masy.200750121

In Situ Formation of a Uniform Distribution of Silver Nanoparticles in PVDF: Kinetics of Formation and Resulting Properties

J. Compton,[*1] *D. Kranbuehl,*[1] *G. Martin,*[2] *E. Espuche,*[2] *L. David*[2]

Summary: Hybrid organic/silver nanoparticle thermoplastic films have been prepared using a single step process where the silver nanoparticles were formed during a cure cycle applied to the film. Figure 1 is a TEM demonstrating the ability of our technique to produce silver nanoparticles in the semi-crystalline polymer Poly(vinylidene fluoride) (PVDF). The current laboratory focus is on characterizing kinetics and particularly the diameter growth and inter-particle distance as a function of time and temperature using the techniques of small-angle X-ray scattering (SAXS), differential scanning calorimetry (DSC), and X-ray diffraction (XRD). Using the Beaucage model, the SAXS data demonstrates that the particle size reaches equilibrium after approximately 70 minutes of curing at 240 °C. This result is also observed in the XRD results where the half width of the diffraction peaks becomes smaller quickly during the initial hour. In a parallel experiment using DSC, the exothermic heat flow increases rapidly during the first hour but does not reach completion until almost 150 minutes.

Keywords: kinetics; metal-polymer complexes; nanoparticles; polyvinylidene fluoride (pvdf); silver

Introduction

Nanoparticles are of increasing interest in the field of material science due to their effect on a range of properties, from thermal properties and stability such as glass transition temperature, melting point, thermal expansion, and material degradation to physical properties such as gas permeability, modulus, strength, and durability.[1–5] A large portion of current literature is based on the incorporation of clays, especially montmorillonites, and their modified derivatives into polymer systems.[6–22] These hybrid systems are challenging to study due to the nature of the nanoparticles which are highly electrostatic sheets with varying chemical compositions and with varying homogeneity and extent of exfoliation within the systems. Many of these systems involve modifying the surface of the particle, particularly in the case of the clay system. This modification introduces a 3rd phase, the interfacial region further complicating studies. All of these factors together make these systems challenging to analyze because it is difficult to isolate individual effects such as the nanoparticles size and to understand how nanoparticle size is improving the material's properties as a whole.

There are currently six methods used for creating nanocomposites: chemical vapor deposition (CVD), electrodeposition, sol-gel synthesis, mechanical crushing, plasma arc and flame pyrolysis methods, and modification of naturally occurring nanomaterials (ie montmorillonite clays, zeo-

[1] Departments of Chemistry and Applied Science, College of William and Mary, Williamsburg, VA 23187, Unites States of America
E-mail: jmcomp@wm.edu
[2] Ingénierie des Matériaux Polymères, IMP, UMR, CNRS 5627, Laboratoire des Matériaux Polymères et des Biomatériaux, Université Claude-Bernard—Lyon I, 69622 Villeurbanne Cedex, France

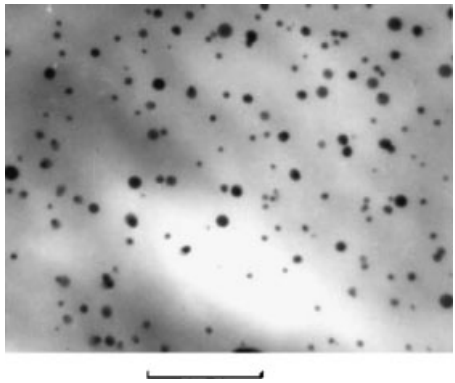

Figure 1.
TEM of 8 wt% Silver in PVDF demonstrating the silver particle dispersion. The scale is representative of 250 nm.

lites, etc).[23] Our approach is unique in that it is an *in situ* process whereby a metal complex is dissolved in the polymer and then it decomposes at a higher temperature to form a uniform dispersion of metal nanoparticles in the polymer.[3,24–26]

It is essential to create a fundamental study to fully understand how individual changes in nanoparticles alter the properties of the material. A direct means of conducting a fundamental study is to have a simpler system than the widely studied montmorillonite-clay systems produce. Here, we propose a system in which the chemical composition is simple, the shape is spherical, the size and distribution is more uniform, and wherein these properties are easily changed. This ideal system allows one to study all of the resulting properties of a nanoparticle material based on the change of a single alteration of the nanoparticle within the system.

Thus far, we have reported the process and characterization of polymer materials with metal and metal oxide nanoparticles using our single stage *in situ* synthesis method.[3,24–26] Our laboratory work so far has dealt with 1) inert nanometer-sized lanthanum oxide nano-clusters and 2) reactive nanometer-sized palladium and silver metal particles and with two polymer systems: poly(amic acids)/polyimides and the high performance thermoplastic polyvinylidene fluoride (PVDF). Our last report focused on showing the breadth of which our technique could be applied to varying particles and matrices.[26] Here, the focus is on the silver-PVDF system and monitoring the kinetics of formation and resulting nanoparticle properties to further the goal of creating a fundamental understanding on factors which control nanoparticle size, shape, and distribution in a polymer matrix.

Experimental Part

Materials

All reagents were used as received from the manufacturer. Poly(vinylidene fluoride) was received from Aldrich Chemical Co. with a M_w of 180,000 and M_n of 71,000. Silver trifluoroacetate (99.99 + %) (AgTFA) and N,N-Dimethylacetamide anhydrous (99.8%) (DMAc) were also received from Aldrich Chemical Co.

Instrumentation

A custom built dry-box was designed for drying the films at ambient temperatures with humidity of approximately 3%.

Films were cured in a General Signal Co. Blue M Electric Forced Air Oven for varying lengths of time at preheated oven temperatures of either 190 °C or 240 °C.

Small Angle X-ray Scattering (SAXS) experiments were run on beam, BM02, at the European Synchrotron Radiation Facility (ESRF) near Grenoble, France. PVDF samples had an exposure time of 1 second and the radiation had an energy of 14 keV.

X-ray Diffraction (XRD) experiments were run using a Bruker SMART APEX II system with an Oxford Cryostream Plus variable temperature system. Amorphous glass templates were placed onto the aluminum stands to ensure there were no peaks from the aluminum and scans were 3 minutes at each of the angles.

Differential Scanning Calorimetry (DSC) experiments were run using a TA Instruments MDSC 2920. The isothermal procedure involved equilibrating at 30 °C for 5 minutes with a modulation of 1 °C/min followed by a jump to either 240 °C or

190 °C which was maintained for 240 min. The post-cure analysis procedure involved 4 steps: initial heating (2 °C/min from 100 °C to 300 °C followed by a 60 min isotherm) to monitor the state of the material and detect if there was ongoing reaction, first cooling (2 °C/min from 300 °C to 100 °C followed by a 60 min isotherm) to monitor recrystalization, final heating (2 °C/min from 100 °C to 300 °C followed by a 60 min isotherm) to monitor the final state of the material after completing the reaction and to compare to the initial heating, and the final cooling (2 °C/min from 300 °C to 100 °C followed by a 60 min isotherm) to compare to the first cooling.

Synthesis of 8 wt% Silver-Poly(Vinylidene Fluoride) Films

PVDF is dissolved in anhydrous DMAc at 20 wt% (1 g of PVDF, 4 g of DMAc) and stirred for 2 hours with gentle heating (~50 °C) in a 20 mL glass scintillation vial with a magnetic stir bar. AgTFA is also dissolved in approximately 0.5 g of DMAc to make a film with 8% Silver by weight (~0.1781 g AgTFA reduces to 0.0870 g Ag). The silver solution is then added to the polymer solution and stirred for another 2 hours.

The homogenous silver-PVDF solution is then poured onto a clean, dust-free glass plate. The film is drawn using a doctor blade set to 0.610 mm and then placed into the level dry box at approximately 3% humidity to dry for a minimum of 12 hours. The film is ready to be cured once it is tact free.

The films were placed into the Blue M Electric Forced Air Oven to remove excess solvent. This treatment consists of increasing the temperature from room temperature to 100 °C over the course of an hour, holding at 100 °C for an hour, and then cooling the oven to room temperature over the course of an hour. The film is removed from the glass plate by placing it into a warm (~45 °C) deionized water bath for approximately 10 min. The film is then dried using Kimwipes and allowed to stand in air. Finally these films were held at 190 °C or 240 °C for varying lengths of time. Afterwards their SAXS and XRD spectrum were taken.

Results and Discussion

DSC

The DSC data (Figure 2) shows an exothermic reaction that occurs at 240 °C that is finished by approximately 150 minutes. The highest rate of reaction is at 17 minutes into the reaction and the halfway point of the reaction is at 38 minutes. The figure displays the exothermic decomposition of the complex and the formation of the nanoparticles. The only other processes that would be occurring at this temperature would be the removal excess moisture/solvent and the melting the polymer; however, these would all be endothermic. The heat generated from the degradation process of the neat metal complex is negligible in comparison to the total heat of reaction of the complex degradation and the particle formation process in the PVDF. As shown in Table 1, the exothermic heat given off from the neat metal complex is an order of magnitude smaller than the heat given off from the polymer-nanoparticle system.

Table 1 also demonstrates the thermal changes of the composite system with respect to the neat polymer system. The addition of silver nanoparticles caused both a decrease in the T_m and the heat of fusion which relates to a decrease in crystallinity as calculated by Kolbeck and Uhlmann using the ΔH_f^o of 100.2 J/g.[27] This suggests the particles inhibit polymer mobility in the vicinity of the nanoparticles.

SAXS

Small-angle X-ray Scattering data is received as radial scattering peaks which is converted into a 2-dimensional scattering plot, as demonstrated in Figure 3. These plots are fitted with the Beaucage model to calculate particle size and distribution.[28] A polymer with no particles will give a distinctive ''background'' signal which can be extrapolated from the lowest q region.

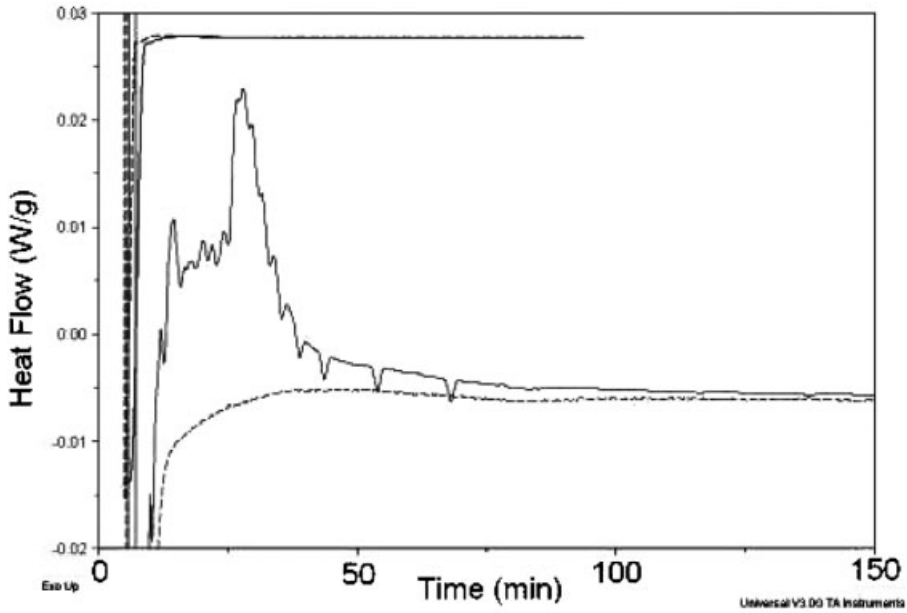

Figure 2.
DSC of 8 wt% Silver in PVDF (top solid curve) and neat PVDF (lower dotted curve) showing heat flow versus time at 240 °C.

This background signal can be subtracted out and the Beaucage model adjusted to fit to the new data which is representative of only the particle scattering.

In Figure 4, the particle size determined from the SAXS spectra versus cure time is analyzed in comparison to the $\alpha(t)$ from the DSC data. The figure clearly shows that particle size changes very little after 70 minutes of cure at 240 °C which is in contrast to the DSC data which shows the reaction continuing until almost 150 minutes into the cure. Both the original data and the background corrected data show the same trend concerning the growth of R_g as a function of time. An explanation for this discrepancy is that the first portion of the DSC data is the particle formation and the second more linear section with a smaller slope is the nanoparticle crystal structure going through an exothermic process to its most stable, ordered configuration.

Also in Figure 4, the interparticle distance determined from the SAXS spectra versus cure time is analyzed in comparison to the $\alpha(t)$ from the DSC data. Interparticle distance does not change much as a function of time which suggests that the particle formation process is due to spinodal decomposition. Our yet unpublished research not presented in this paper

Table 1.
Silver PVDF Film MDSC Data from 240 °C Isothermal Hold and Post Ramp Analysis of Thermal Properties.

System	240 °C Isotherm		Post Ramp Analysis		
	ΔH	Heat Flow Max	ΔH	T_m	% Crystallinity
Neat PVDF	—	—	47.4 J/g	169.1 °C	47.3
PVDF-Ag	43.9 J/g	18.2 min	43.4 J/g	162.1 °C	43.3
Neat AgTFA	5.8 J/g	6 min	—	—	—

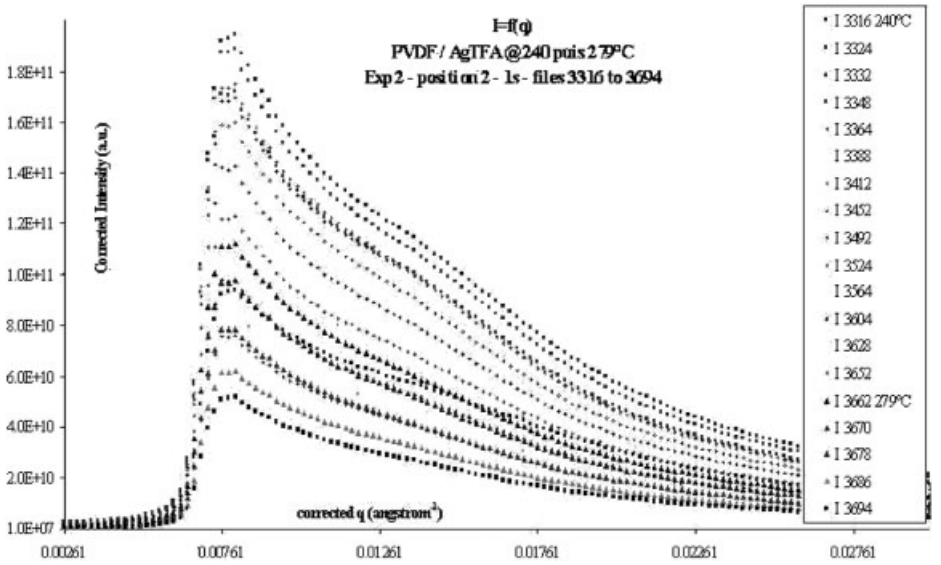

Figure 3.
SAXS data demonstrating the scattering due to silver nanoparticles in PVDF over time at 240 °C.

from our other systems also supports that similar systems undergo spinodal decomposition based on their SAXS scattering pattern versus time.

XRD

Since the films studied have silver nanoparticles, X-ray diffraction can be used to monitor the formation of the crystalline structures of both the particles and the polymer as shown in Figure 5. The 100 degree treated polymer films were partitioned into smaller pieces and cured for varying times to study the change as a function of cure time. At 1 minute of cure time, there are no noticeable crystalline silver peaks in the diffractogram. By minute 2, crystalline silver peaks clearly emerge from the baseline at $2\theta = 38.2$, 44.3, 64.4, 77.3, 81.5, 110.5, and 114.9. As cure time

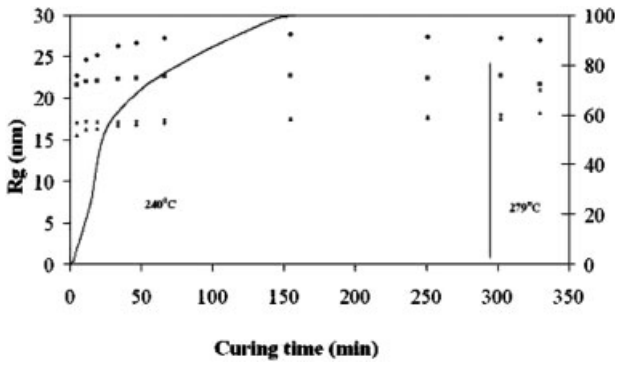

Figure 4.
SAXS Data demonstrating the increase in both D_{inter} (lower two series of data points) and R_g (higher two series of data points) as a function of time. Both the original Beaucage fit and the background corrected fit data is included, showing the same trends. Also shown is the $\alpha(t)$ of the reaction (solid curve).

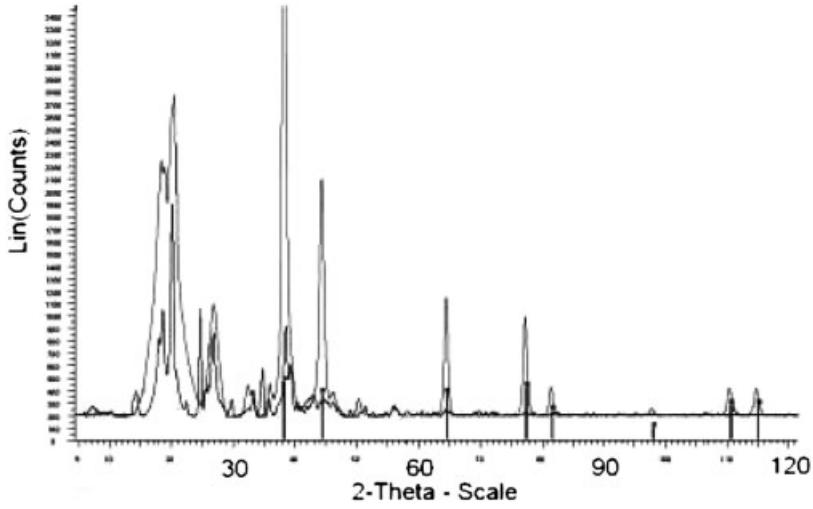

Figure 5.
XRD of 8% Ag in PVDF at 1 minute and 50 minutes of cure. The lower peaks are the 1 minute cure time whereas the higher less sharp peaks are the 50 minute sample. Vertical lines are the standard crystalline silver diffraction peaks.

increases, the height of the silver peaks increases and the peaks become narrower as demonstrated in Figure 6.

The particle size can also be investigated using the Debye-Scherrer formula which is an extension of Bragg's Law

$$t = \frac{0.9\lambda}{\mathrm{B}\cos\theta},$$

where t is the particle thickness, λ is the wavelength of incident radiation, B is the full half height width (in radians), and θ is the position of the maximum in the diffraction peak. The thickness of the particles is assumed to be roughly equivalent to the diameter of the particles and is easily calculated for varying cure times and at varying diffraction peaks. Table 2 shows

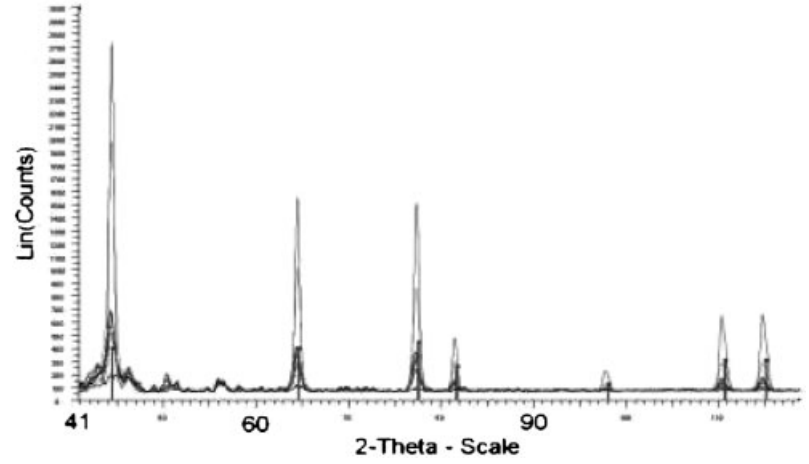

Figure 6.
XRD of 8% Ag in PVDF at 1, 2, 3, 5, 7, 10, 50, and 480 minutes of cure. The lower peaks are the lower cure times and the peaks increase in height but narrow with increasing cure time. Red lines are the standard crystalline silver diffraction peaks.

Table 2.
Silver PVDF Film XRD Peak Analysis using the Debye-Scherrer formula to determine particle thickness.

2theta	77.319	2theta	110.42
1 deg (mm)		1 deg (mm)	
cure time	t (nm)	cure time	t (nm)
50	12.487999	50	13.4469848
10	11.5959991	10	12.3890251
7	11.948808	7	12.4859956
5	11.9702312	5	12.8444243
3	11.8744268	3	10.6178839
2	8.76023812	2	13.7570671
2theta	81.465	2theta	114.831
1 deg (mm)		1 deg (mm)	
cure time	t (nm)	cure time	t (nm)
50	13.8417487	50	14.7663211
10	13.5790545	10	14.1664393
7	12.3679767	7	14.5514463
5	16.7597949	5	14.2824845
3	13.6729126	3	11.2098432
2	12.8869625	2	14.9087719

the particle thickness as a function of time using this equation. As particles become larger, the error associated with the inherent diffraction width is a larger factor in comparison to the diffraction from small particles.

In addition, the polymer crystalline structure seems to change during the cure cycle as evidenced in Figure 5. One minute into the cure, there are numerous polymer crystalline peaks most of which are sharp in contrast to the later cure times. The number of polymer peaks remains fairly numerous (~13 identifiable peaks) through minute 10 of the cure. 50 minutes into the cure, the number of peaks has dropped significantly to around 9 identifiable peaks and these peaks have a broader contour, suggesting a wider distribution of crystallite structures and intraplanar distances.

Conclusions

A uniform distribution of silver nanoparticles is formed in the PVDF system using a single-step *in situ* process. SAXS, DSC, and XRD have been used to monitor the particle formation. At 240 °C, the nanoparticles form within a few minutes with a diameter close to their final diameter. These results suggest the process is spinodal decomposition. A small increase in size occurs over the next 60 minutes. Verification of similar spinodal processes is being pursued in work on other combinations of nanoparticles and polymers.

Acknowledgements: We are indebted to NSF (CHE-0443345) and the College of William and Mary for the purchase of the X-ray equipment.

[1] Z. Ahmad, J. E. Mark, *Chemistry of Materials* **2001**, *13*, 3320–3330.
[2] L. J. Bian, X. F. Qian, J. Yin, Z. K. Zhu, Q. H. Lu, *Journal of Applied Polymer Science* **2002**, *86*, 2707–2712.
[3] D. S. Thompson, D. W. Thompson, R. E. Southward, *Chemistry of Materials* **2002**, *14*, 30–37.
[4] R. A. Zoppi, S. Das Neves, S. P. Nunes, *Polymer* **2000**, *41*, 5461–5470.
[5] L. Tröger, H. Hinnefeld, S. Nunes, M. Oehring, D. Fritsch, *J. Phys. Chem. B* **1997**, *101*, 1279–1291.
[6] T. Agag, T. Koga, T. Takeichi, *Polymer* **2001**, *42*, 3399–3408.
[7] B. J. Chisholm, R. B. Moore, G. Barber, F. Khouri, A. Hempstead, M. Larsen, E. Olson, J. Kelley, G. Balch, J. Caraher, *Macromolecules* **2002**, *35*, 5508–5516.
[8] Y. Fukushima, S. Inagaki, *Journal of Inclusion Phenomena* **1987**, *5*, 473–482.
[9] Y. Fukushima, A. Okada, M. Kawasumi, T. Kurauchi, O. Kamigaito, *Minerals* **1988**, *23*, 27–34.
[10] J. W. Gilman, *Applied Clay Science* **1999**, *15*, 31–49.

[11] A. Gu, F. C. Change, *Journal of Applied Polymer Science* **2000**, *79*, 289–294.
[12] A. Gu, S. W. Kuo, F. C. Chang, *Journal of Applied Polymer Science* **2001**, *79*, 1902–1910.
[13] S. H. Hsiao, G. S. Liou, L. M. Chang, *Journal of Applied Polymer Science* **2001**, *80*, 2067–2072.
[14] Y. Kojima, A. Usuki, M. Kawasumi, A. Okada, Y. Fukushima, T. Kurauchi, O. Kamigaito, *Journal of Materials Research* **1993**, *8*, 1185–1189.
[15] Y. Kojima, A. Usuki, M. Kawasumi, A. Okada, T. Kurauchi, O. Kamigaito, *Journal of Polymer Science, Part A: Polymer Chemistry* **1993**, *31*, 983–986.
[16] T. Lan, P. D. Kaviratna, T. J. Pinnavaia, *Chemistry of Materials* **1994**, *6*, 573–575.
[17] P. C. LeBaron, Z. Wang, T. J. Pinnavaia, *Appl. Clay Sci.* **1999**, *15*, 11–29.
[18] A. B. Morgan, J. W. Gilman, C. L. Jackson, *Macromolecules* **2001**, *34*, 2735–2738.
[19] H. L. Tyan, Y. C. Liu, K. H. Wei, *Chem. Mater.* **1999**, *11*, 1942–1947.
[20] H. L. Tyan, Y. C. Liu, K. H. Wei, *Polymer* **1999**, *40*, 4877–4886.
[21] K. Yano, A. Usuki, A. Okada, *Part A: Polymer Chemistry* **1997**, *35*, 2289–2294.
[22] K. Yano, A. Usuki, A. Okada, T. Kurauchi, O. Kamigaito, *Part A: Polymer Chemistry* **1993**, *31*, 2493–2498.
[23] M. Freemantle, *Chemical and Engineering News* **2006**, *84*, 28–29.
[24] E. Espuche, L. David, C. Rochas, J. L. Afeld, J. M. Compton, D. W. Thompson, D. Thompson, Scott, D. E. Kranbuehl, *Polymer*, **2005**, *46*, 6657–6665.
[25] J. Compton, D. Thompson, D. Kranbuehl, S. Ohl, O. Gain, L. David, E. Espuche, *Polymer* **2006** (In Print).
[26] E. Espuche, L. David, J. L. Afeld, J. M. Compton, D. E. Kranbuehl, *Macromol. Symp.* **2005**, *228*, 155–165.
[27] A. G. Kolbeck, D. R. Uhlmann, *J. Polym Sci, Polym Phys. Ed.* **1977**, *15*, 27–42.
[28] G. Beaucage, D. W. Schaefer, *Journal of Non-Crystalline Solids* **1994**, *58*, 1551–1560.

